On-Orbit Meteor Impact Monitoring Using CubeSat Swarms

Ravi teja Nallapu
Space and Terrestrial Robotic Exploration Laboratory,
Department of Aerospace and Mechanical Engineering, University of Arizona
Himangshu Kalita
Space and Terrestrial Robotic Exploration Laboratory,
Department of Aerospace and Mechanical Engineering, University of Arizona
Jekanthan Thangavelautham
Space and Terrestrial Robotic Exploration Laboratory,
Department of Aerospace and Mechanical Engineering, University of Arizona

ABSTRACT

Meteor impact events such as Chelyabinsk are known to cause catastrophic impacts every few hundred years. The modern-day fallout from such event can cause large loss of life and property. One satellite in Low Earth Orbit (LEO) may get a glimpse of a meteor trail. However, a swarm constellation has the potential of performing persistent, real-time global tracking of an incoming meteor. Developing a swarm constellation using a fleet of large satellites is an expensive endeavor. A cost-effective alternative is to use CubeSats and small-satellites that contain the latest, onboard computers, sensors and communication devices for low-mass and low-volume. Our inspiration for a swarm constellation comes from eusocial insects that are composed of simple individuals, that are decentralized, that operate autonomously using only local sensing and are robust to individual losses.

This work illustrates the design of a constellation of large number CubeSats in LEO at altitude of 400 km and higher, referred to as a swarm, in order to monitor the skies above entire North America. Specifically, this work extends the capability of a 3U CubeSat mission known as SWIMSat, by converting it into a swarm, to monitor the region over North America at an altitude of 140 km.

The design of a swarm in LEO faces multiple challenges such as the limited field of view of the spacecraft-instrument and resulting observation quality. The design is further complicated by the fact that in order to enable triangulation of the meteor event, the entire region of interest should be observed by at least two nodes. Due to the complicated nature of the problem, an analytical treatment is challenging. This work aims to solve these challenges by the reducing the problem into designing a circular Walker-Delta constellation in LEO, with repeating ground track orbits. The approach employed in the work is as follows: First, an optimal orbit inclination is determined by propagating the orbit forward in time. Here a cost-function which is the weighted sum of percentage area observed, and the observed duration is formulated. The optimal inclination is determined based on the RAAN averaged cost function of the inclinations. Then to ensure that the orbits repeat periodically, the altitudes of repeat ground track (RGT) orbits possible in LEO are determined, and the corresponding field of view of the instrument on the node is determined analytically from its viewing geometry. A circular Walker-Delta constellation with these defined RGT altitudes and optimal inclination is then designed, by simulating its design space. The minimum sized swarm is then noted, and its performance is observed. The lifetime of a node is estimated, along with the amount of ΔV required to maintain the orbit. Finally, the effect of a node failure on coverage is studied using dynamic simulations.

Results indicate that 4 different minimum sized swarms are possible in the LEO, each corresponding to an RGT orbital altitude. The minimum size varied from 180 nodes at an altitude of about 1,660 km to 1365 nodes at an altitude of 540 km, such that every point on the target grid was observed by at least 2 spacecrafts. The current work contributes to the existing literature by first presenting the importance of realizing a constellation to monitor meteor impacts using small satellites. Then, an optimal swarm is designed by using state-of-art constellation design tools. In addition, several key challenges and relevant literature are presented, and finally, a toolbox of computational routines to design constellations is developed.

1. INTRODUCTION

Meteor impacts pose a severe threat to the modern civilization. Meteors larger than 10 m are known to release energy on the order of hundreds of kilotons during impact. The atmospheric explosion of the Chelyabinsk meteor in 2013, where about 500 kilotons of energy (nearly 33 times the energy released from Hiroshima atomic bomb) was released during its airburst [1], serves as an indicator of the potential hazard of these events. Additionally, the database of near-

Earth objects maintained by NASA-JPL, reports that at least 600 meteor events with energies greater than 0.1 kilotons were recorded in the last 30 years [2]. The modern-day fall out of such impact events can be catastrophic. Therefore, there is a strong need to have a real-time monitoring network that can provide an advance warning, and help us prepare for countermeasures. To this effect, the SWIMSat (Space based Wide-angle Imaging of Meteors Satellite) mission was proposed as a first step towards realizing such a network [3]. The SWIMSat mission consists of two 3U CubeSat, in low Earth orbit (LEO) at an altitude of 450 km. The payload of SWIMSat is a wide-angle camera with an angular field of view (AFOV) of 143 deg. The different subsystem components of the SWIMSat spacecraft are shown in Fig.1.
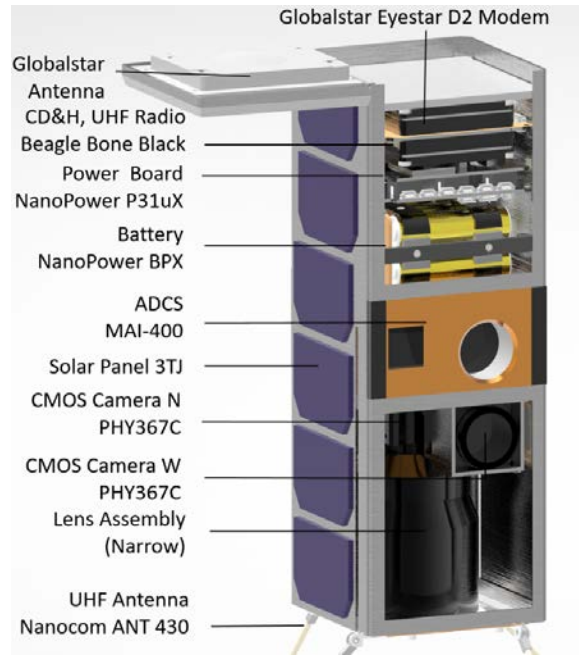

Fig. 1. A sectional view of the SWIMSat spacecraft revealing its different subsystem components.

Once, a meteor enters the field of view (FOV) of SWIMSat, a spacecraft uses its onboard vision processing algorithms to detect the event and then uses its attitude determination and control system to track the meteor [3, 4].   A second spacecraft is notified and both track and determine the position, velocity and acceleration of the object. The obtained data is then downlinked to a ground station, with its onboard UHF communications system, for further analysis. These operations of SWIMSat are summarized in Fig.2.
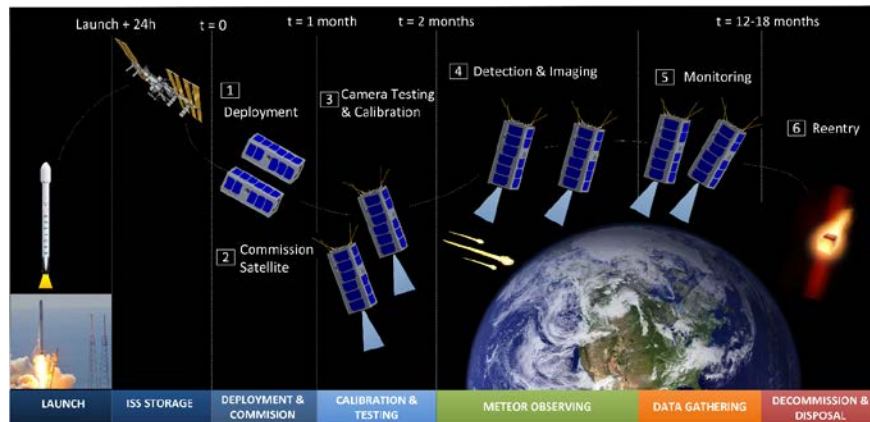

Fig. 2. The concept of operations of the SWIMSat mission.

Multi-point observation of the meteor with two or more spacecraft can provide a lot more critical information including radiance, position, altitude, length, diameter, geocentric velocity, heliocentric trajectory, photometric mass [5, 6, 7, 8]. Importantly, using multiple spacecrafts, a constellation can be designed to provide uninterrupted coverage of the target region. A constellation of satellites also adds the benefit of tolerance for single point failures. Due to their low cost, CubeSats or small satellites are the ideal platform to realize this constellation.

This concept of multi-node synergy is commonly found in swarms of eusocial insects, where decentralized individuals operate autonomously with local sensing in order to accomplish complex common objectives. For this reason, the meteor observing constellation will be referred as a swarm constellation, and the individual spacecrafts are referred to as the nodes. This work describes the design of a swarm constellation constructed from the SWIMSat spacecraft as its nodes. The swarm will monitor the skies above North America and its surroundings for meteor events. The constellation designed has the following 2 objectives:
1. The constellation must continuously monitor the region above North America at an altitude of 140 km.
2.   Any point in this region must be observed by at least 2 nodes at all points of time.
The first objective is based on the observation that most meteor trails are observed between altitudes 140 km to 70 km altitudes [5]. The second objective enables the swarm to triangulate the meteor event and track its above mentioned dynamic properties.

The design of this constellation faces multiple challenges. First, a very small portion of the Earth is visible from the LEO altitudes while the latitude-longitude range of the target region is large. This is further aggravated by objective 1, where the target observation region is at an altitude of 140 km above the Earth's terrain. The second challenge of having continuous 2-satellite coverage over the entire target, which complicates the design space. Due to a large number of free variables and complex structure of this problem, analytical techniques cannot be readily applied.

In this work, the above challenges are tackled using computational tools, where simulations and analytical tools are used to simplify and observe a design space. We proceed by first obtaining the orbital and observing properties of a seed spacecraft, based on a computation grid. To avoid collision issues with a large number of spacecrafts, and also to simplify the design, only circular orbits are considered for the design. For their repeating properties, repeat ground track (RGT) orbits are used. Once the orbit of the seed spacecraft is fixed, the swarm is then designed by using a Walker-Delta constellation from the seed. The design space is then analyzed for the coverage parameters to obtain the minimum sized swarm which yields an uninterrupted 2-satellite coverage of the target region. Additional practical concerns, such as the life of the nodes, station keeping ΔV, and performance under single point failures is also analyzed. The orbit and constellation simulations were performed using the software Satellite Tool Kit (STK) and the results were processed and analyzed in MATLAB. In the following sections we present background, followed by methodology, results, discussion, conclusions and future work.

2.   BACKGROUND

This section provides a brief background of the problem at hand along with the tools used to perform swarm constellation design work. This information is required to design the orbit of a single node and construct a constellation. We discuss the orbital elements, repeat ground track orbits, viewing geometry, the Walker-Delta constellations, and required station keeping. Additionally, a brief description of STK and tools used in designing a Walker-Delta constellation are also provided.

Orbit elements: From Kepler's laws of planetary motion, the motion of an orbiting satellite under influence of Earth's gravity alone is an ellipse, and this motion can be described by 6 parameters: Semi-major axis (a), eccentricity (e), inclination (i), right ascension of the ascending node or RAAN (Ω), argument of perigee (ω), and the true anomaly (ν_0). These elements can be found in Fig.3. These parameters are defined in an Earth centered inertial (ECI) reference frame with origin at the Earth's center. The axes of ECI frame are defined as follows: the x-axis points towards the vernal equinox, the z-axis is the in the direction of the Earth's North pole, and the y-axis completes the right-hand rule. The elements in the ECI frame are then defined as follows:
-    Semi-major axis, (a): The distance of any of the apsis of the ellipse from its center.
-    Eccentricity, (e): Eccentricity is an indicator of the elongation of the orbit. The value of e lies in $[0,1)$ for an orbiting spacecraft, where $e = 0$ represents the special case of a circular orbit.
-    Inclination, (i): The angle between the z-axis of the ECI frame, and the normal vector to the orbital plane
-    RAAN, (Ω): The ascending node is the point where the satellite ascends the equatorial plane of the Earth. RAAN then is defined as the longitude of the node as measured from the x-axis of the ECI frame.

-   Argument of perigee, (ω): The argument of perigee is the longitude of the periapsis of the ellipse, as measured from the ascending node in the counter clockwise direction. This parameter is not used for circular orbits.
-   True anomaly, (v_0): The true anomaly is the longitude of the current position of the satellite measured counter clockwise from the orbital periapsis.
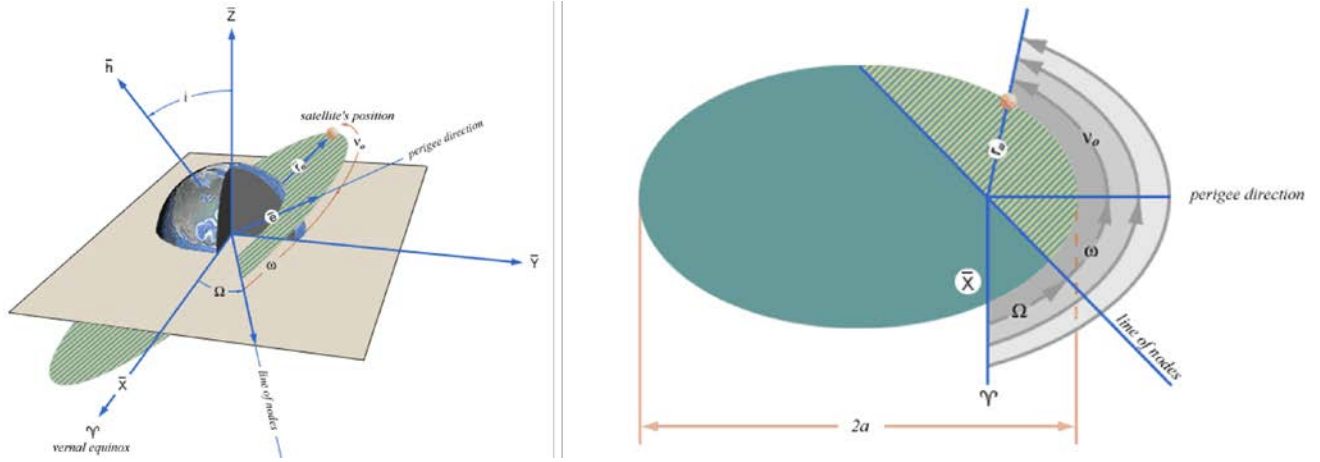

Fig. 3. Orbital elements of a satellite's motion around Earth. The image on the left shows the 3-dimensional motion of the satellite around Earth in the ECI frame, the image on the right shows the satellite path as seen in the orbit plane. Image courtesy: https://spaceflight.nasa.gov

The velocity of the satellite at any point on the orbit is found from the Kepler's first law as [9]:

$$V = \sqrt{\frac{\mu}{r}\left(2 - \frac{1-e^2}{1+e\cos v_0}\right)} \tag{1}$$

Where V is the magnitude of the velocity of the spacecraft in the ECI frame, μ is the gravitational parameter of the Earth, and r is the position of the spacecraft with respect to the Earth's center. The implication from (1) is that, for an eccentric orbit ($e \neq 0$), the speed of the spacecraft varies with its location on the orbit. Since a Walker-Delta, constellation uses multiple satellites in a single orbit plane, we can run into satellite-satellite collisions on an eccentric orbit, according to (1). For this reason, we only use circular orbits ($e = 0$) for the swarm constellation. The magnitude of the spacecraft position with respect to Earth center is expressed as:

$$r = R_E + h \tag{2}$$

Where, R_E is the radius of the Earth, and h is the altitude above the Earth's surface. An orbit which lies in the region between $h = 350$ km to $h = 2000$ km is usually referred to as a low Earth orbit (LEO) and is an ideal region to place a CubeSat in orbit.

Repeat ground track orbits: The repeat ground track (RGT) orbits are those orbits whose projections on the surface of the Earth, or ground tracks, repeat regularly for every j orbits of the satellite around Earth [10, 11]. The RGT orbits are also commonly used for Earth observations due to their regular repeat cycles [12, 13, 14]. If the Earth is assumed to be a perfect sphere, then repeat ground track orbits are possible if the ratio of the orbital period of the satellite to Earth's sidereal rotation can be expressed as a ratio of 2 integers. Using Kepler's third law, this can be expressed as:

$$\omega_E \sqrt{\frac{a^3}{\mu}} = \frac{k}{j} \tag{3}$$

Where, ω_E is the angular velocity of Earth's sidereal rotation, and k and j are any 2 positive integers. (3) constraints the semi major axis of the satellite to have an RGT orbit. However, (3) only applies if no perturbations to the spherical gravity are considered. The dominating source of perturbation from the spherical gravity is produced by Earth's oblateness which causes the RAAN to drift over the time and is known as the j_2 effect. Vallado and McClain [9]

provides an iterative algorithm to find the RGT orbits under the j_2 effect, which is used in this work to find the working altitude of the spacecraft nodes. (3) will provide the initial value for the algorithm used.

Viewing geometry: The viewing geometry of the spacecraft node observing the Earth for meteors is presented in Fig. 4. The target region where meteor trails begin is at an altitude h_m. From an altitude h, the horizon is captured with in a semi-horizon angle of ρ. If the spacecraft observes a point on the target with an elevation angle ε, the nadir angle η can be determined from spherical trigonometry as [10, 11]:

$$\sin \eta = \cos \varepsilon \sin \rho \tag{4}$$

For the swarm constellation being designed, we assume that the nodes have a conical field of view, which is pointed towards the nadir to avoid motion blur. Therefore, the nadir angle, in this case, is also the half cone angle of the spacecraft camera. The semi-horizon angle in (4) can be determined by:

$$\sin \rho = \frac{R_E + h_m}{R_E + h} \tag{5}$$

The elevation angle effects the quality of observation. Observations at $\varepsilon = 0$ deg (at the horizon) will be completely distorted, while those at $\varepsilon = 90$ deg (nadir point) are undistorted. A lower bound of $\varepsilon = 25$ deg is used in the current design.
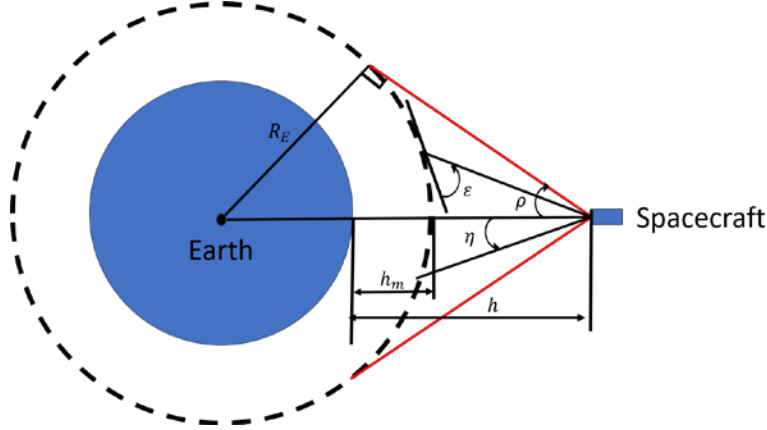

Fig. 4. Viewing geometry of the meteor observing node

Walker-Delta constellation: A Walker-Delta constellation creates a constellation of uniformly distributed spacecrafts. Due to their symmetry, the Walker-Delta patterns are popularly used for designing constellations for remote sensing missions [10, 11]. The design of a Walker-Delta constellation begins after the orbit of a single node spacecraft is identified. This first node is referred as the seed for the constellation. The constellation is then created by taking placing N_{sp} copies of the seed in the same orbital place, which are separated by $\frac{360}{N_{sp}}$ deg in true anomaly; and N_p copies of such orbital planes, each separated in RAAN by $\frac{360}{N_p}$ deg. The total number of satellites in the constellation, therefore is:

$$T = N_p N_{sp} \tag{6}$$

The design of a Walker-Delta constellation is completed by specifying the phase difference between adjacent planes, $\Delta\phi$. The phase difference is measured as the angle in the direction of motion which is measured from the ascending node to the nearest satellite when the satellite in the immediate westward plane is at its ascending node. The phase difference is expressed as:

$$\Delta\phi = F \frac{360}{T} \tag{7}$$

Where F is an integer in $[0, N_p - 1]$. The design of a Walker-Delta constellation is specified by the notation: $i: T/N_p/F$. The geometry of a Walker-Delta constellation $90: N_p N_{sp}/N_p/F$ nodes is shown in Fig. 5.
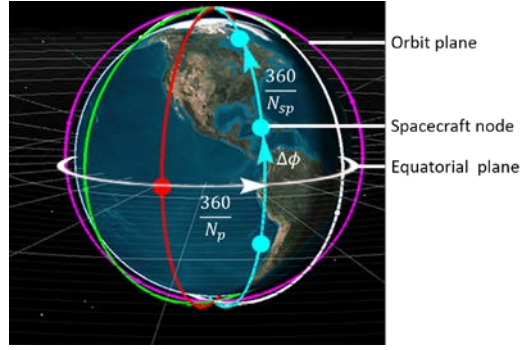
Fig. 5. The geometry of a Walker-Delta constellation of the pattern 90: N_p $N_{sp}/N_p/F$ showing different angles and their distributions.

Station keeping: Station keeping is a spacecraft maneuver to maintain its orbit, which otherwise decays due to perturbations and is accomplished by using onboard fuel. The magnitude of change in spacecraft's velocity, ΔV during the maneuver is used as a proxy to the fuel consumed by the maneuver. The aerodynamic drag is considered as the dominant perturbation of satellite decay in LEO. Wertz [10] provides an analytical formula to estimate the ΔV required per orbit for the station keeping maneuver under aerodynamic drag, which is given by:

$$\Delta V_{rev} = \pi \left(\frac{C_D A}{m}\right) \rho_{atm} a V \tag{8}$$

The subscript 'rev' in (8) indicates that ΔV computed is per 1 revolution of the spacecraft or 1 orbit. The parameter C_D denotes the drag coefficient, A denotes the effective spacecraft area exposed to drag, m denotes the spacecraft mass, ρ_{atm} denotes the atmospheric density at the spacecraft's altitude, and V is the spacecraft's velocity computed from (1).

Satellite Tool Kit: *The Satellite Tool Kit,* (STK) is a space mission design software developed by *Analytical Graphics, Inc*. The software provides mission designers with high fidelity environment models and trajectory propagation algorithms. STK also comes with routines to convert a single seed satellite into a Walker-Delta constellation of desired parameters and study the coverage performance for a defined target grid. Additionally, STK also provides an estimate of the orbital life. The computed lifetime in STK is the time taken for the periapsis of the orbit to decay to below 64 km, due to atmospheric drag, and solar radiation pressure.

In the present work, STK was used to study the swarm coverage of the target region above North America at an altitude of 140 km. The coverage is judged by a 2-satellite coverage Figure of Merit (FoM), such that constellation is:
- Successful, if every point in the target grid is observed by at least 2 spacecrafts
- Failure, if every point in the target grid is not observed by at least 2 spacecrafts

The satisfaction duration is also noted for the constellation, which is the duration for which a given constellation was successful. From the above-mentioned objectives, the target constellation should be successful for the entire simulation duration to provide continuous coverage.

Finally, STK also provides a subroutine known as the *Analyzer*, which is useful for studying the performance by changing the design parameters. In the present study, the *Analyzer* module was used to note the figure of merit, and satisfaction duration of the Walker-Delta constellation, by varying N_p and N_{sp}. The optimal constellation was then determined as the constellation with minimum T which satisfied the two above defined objectives.

3. METHODOLOGY

This section describes the procedure used to design a minimum sized Walker-Delta constellation which enables the swarm to observe the target region completely and continuously by at least 2 satellites. We proceed by defining the grid above the target region. We then find an optimal inclination which maximizes a cost function that depends on the access area and observed duration. The inclination is then used to identify the RGT orbits in LEO for the seed node. The Walker-Delta constellations are then constructed from these seed nodes, and the minimum sized swarms are then identified for different RGT orbits. The lifetimes, and station keeping ΔV is also estimated for these orbits.

Target region: In this study, the target observation region is the region above North America at an altitude of 140 km. The North American terrain contains discontinuous and spread out land masses. In the present study, 2 large rectangular latitude-longitude grids over North America, and its surroundings were used to study the swarm coverage. Both the grids used are marked by the following latitude-longitude bounds:

Table 1: Latitude-longitude bounds of the rectangular grids above North America used in the current work.

Parameter	Value (deg)	Rounded value (deg)	Enforcing Yerrain
Minimum latitude	7.20	6	Isla Jicarta, Panama
Maximum latitude	83.68	85	Greenland
Minimum longitude	172.45	171	Attu Island, Alaska, USA
Maximum longitude	-11.424	350	Greenland

A visual representation of this latitude-longitude box is shown in Fig. 6. and is shaded red.

Fig. 6. Latitude-longitude boundaries of the target area (North America) shown shaded in red.

The target observation region was created at an altitude of 140 km above the terrain of the boundary presented in Fig. 6 which measured a physical area of about 1.2×10^8 km^2. Two grids were defined on this target region based on the grid spacing between latitudes and longitudes: a fine grid with a grid spacing of 0.5 deg, and a coarse grid with a grid spacing of 5 deg, which are shown in Fig. 7. The fine grid was used to obtain the optimal orbit inclination while the coarse grid was used to study the coverage of the constellations.
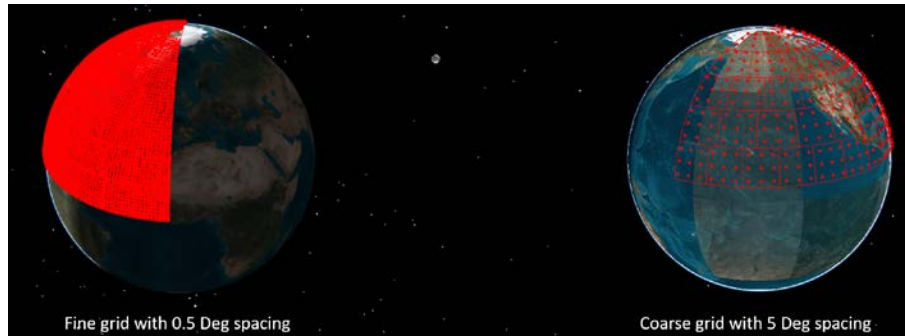

Fig. 7. The computational grids defined on the target region used in the present work. The fine grid structure (left) is observed from the eastern border, while the coarse grid structure (right) is observed from the western border. Both the grids are at an observation altitude of 140 km above the target terrain.

Optimal inclination: To determine the optimal orbit inclination, the orbit of the seed spacecraft was propagated at a test altitude, $h_t = 400$ km. From (4), a value of $\eta = 60.6$ deg, will provide an $\varepsilon = 25$ deg at this altitude. The orbit of the seed node was propagated multiple times by varying the inclination and RAAN in discrete steps. The parameters used for this trade study are presented in Table 2.

Table 2. Trade study parameters used to search for the optimal inclination.

Parameter	Value
Target height, h_t	400 km
Minimum elevation angle, ε	25 deg
Sensor half cone angle, η	60.634 deg
Inclination search range, i	[70, 90] deg
Inclination step size, Δi	2 deg
RAAN search range, Ω	[0, 180] deg
RAAN step size, $\Delta\Omega$	5 deg
Orbit propagation duration	24 hrs
Time step	60 seconds

These orbits were propagated in STK and the percentage of the fine grid area observed by the spacecraft's sensor for each simulation, and its total target access duration was noted. Since Ω is a uniformly distributed quantity in the Walker-Delta formulation, the results obtained from the above study were averaged over Ω, to yield the relation between inclination and single satellite coverage parameters. These results are presented in Fig. 8.
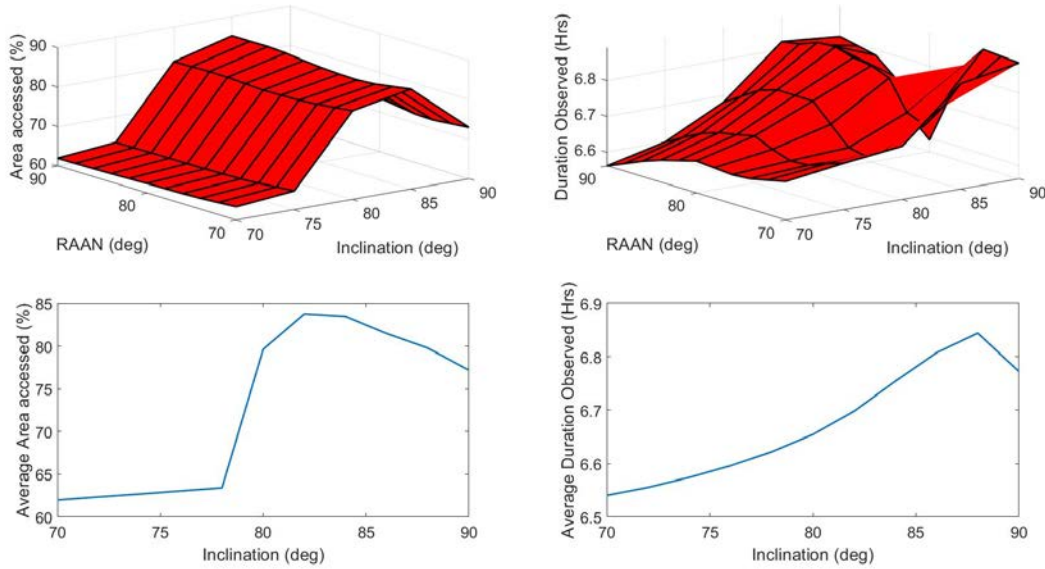

Fig. 8. Coverage parameters used for finding the optimal inclination of the seed node. The surface plots above are the results of trade study showing the variation of the coverage parameters based on inclination and RAAN. The bottom plots contain the RAAN averaged coverage parameters.

The optimal inclination should maximize both the area observed and the duration of observation. Therefore, to find the optimal inclination from these 2 coverage parameters, a cost function for each inclination was defined as follows:

$$J_l = \frac{1}{2}\left(\frac{<\% \ Area \ observed_l>_\Omega}{100} + \frac{<Duration \ observed_l>_\Omega}{\max_l <Duration \ observed>_\Omega}\right) \quad (8)$$

Where, the subscript 'l' denotes the lth inclination, and the notation $<.>_\Omega$ denotes that the enclosed quantity is a RAAN averaged quantity. The variation of the cost function with the inclination is presented in Fig. 9.
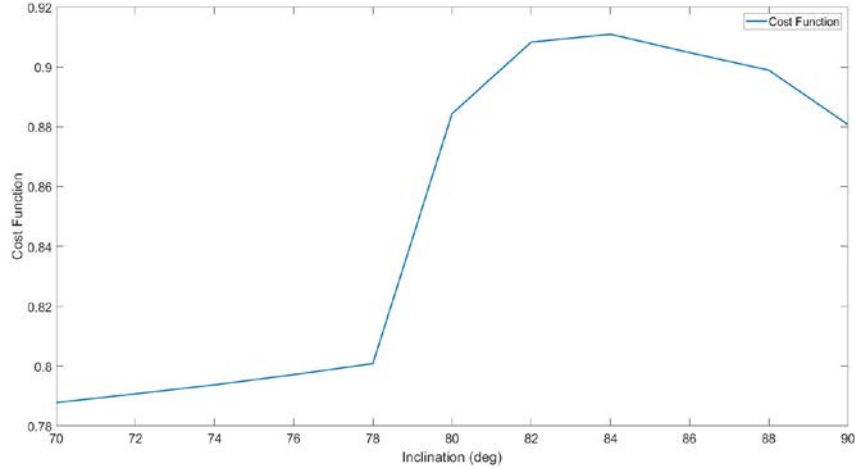
Fig. 9. Dependence of the cost function on the inclination of the seed node.

The optimal inclination is determined from Fig. 9 as the inclination for which the cost function is maximized. In this case, the optimal inclination is $i_{opt} = 84$ deg, yielding a maximum cost function of $J_l = 0.9109$.

RGT Orbits. Once the optimal inclination is known, the altitudes of the RGT orbits are be determined using the Algorithm 71 in [9] for 10 iterations. The initial guesses for this algorithm were determined from (3). In the LEO altitudes corresponding to 350 to 2000 km, four RGT orbits are possible which occur within 1 day. The RGT orbits, their corresponding initial guesses, and the sensor half cone angle at these altitudes required for observing with $\varepsilon = 25$ deg are presented in Table 3. The Walker-Delta constellations were designed for these 4 seed orbits.

Table 3. RGT orbits with $i = 84$ deg, possible in LEO and their corresponding sensor angles.

Resonance		Initial RGT altitude (km)	RGT altitude with j_2 compensation (km)	η (deg)
k	j			
1	12	1670	1660	47.3
1	13	1250	1240	50.8
1	14	880	871	54.6
1	15	554	544	58.6

Walker-Delta Constellation Design. The previous subsections have described the methods used to determine orbital altitude and inclination. These parameters are now sufficient to design the Walker-Delta constellations with circular orbits. In this work, the effect of the phasing parameter F is not considered, and a value of $F = 1$ is used, which reduces the design space of the Walker-Delta constellation to 2 parameters: N_p and N_{sp}. A trade study was then setup where the coverage was studied for different values N_p and N_{sp}. A large initial value for N_p and N_{sp} was selected, such that there was complete satisfaction duration. Then the coverage was observed by reducing these parameters with a step size of 1. To reduce the computation time, the range of design space was kept limited enough to observe the decay from the 100 % satisfaction plateau. The 2 Satellite coverage described in the previous section is used as the figure of merit, and the satisfaction duration over the coarse grid is noted. The minimal constellation had the lowest value of T, which provided complete satisfaction duration during a simulation period of 24 hrs. This trade study was done for all the four RGT altitudes in Table 3, and the corresponding minimal constellations are noted.

Lifetime and Station Keeping ΔV. As mentioned previously, the decay of orbits in LEO is dominated by aerodynamic drag. The lifetimes of the spacecraft in the 4 RGT orbits were found from STK. If the spacecraft nodes carry an onboard propulsion system, then this decay can be prevented. The ΔV required to the maintain the orbit for 1 year is noted using (8). The spacecraft parameters used for this estimation are presented in Table 4. The atmospheric density was estimated using the patched exponential atmospheric model presented in [9].

Table 4: Trade study parameters used to search for the optimal inclination.

Parameter	Value
Mass, m	4 kg
Area of exposure, A	436 cm^2
Drag coefficient, C_D	2.2
Reflectivity coefficient, C_R	0.2

Single point failures: For the 4 minimal swarm constellations designed, a single point failure was simulated by removing a node from the constellation. The satisfaction duration under failures is are for each case.

4. RESULTS & DISCUSSION

This section presents the results of the Walker-Delta constellation design described in the previous section. The design space for the Walker-Delta constellation is presented here, and the minimal swarm size is noted from the response of the satisfaction duration. The orbital life and station keeping requirements for each design are noted. Additionally, the performance under single point failures is also presented.

Minimal Constellation at $h_1 = 1660$ km. The response of the satisfaction duration of multiple swarms possible at $h_1 = 1660$ km is presented in Fig. 10. The design space of N_p and N_{sp} was limited to the range $[10, 18]$, to save computation time.
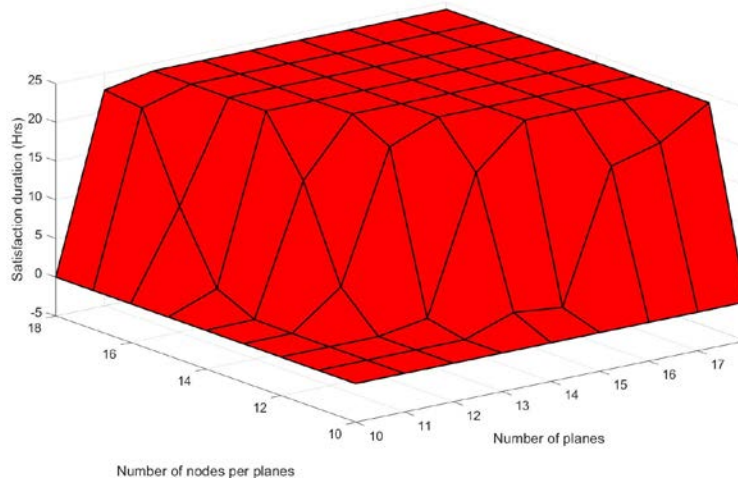

Fig. 10. Satisfaction duration of the multiple swarms possible at $h_1 = 1660$ km.

As seen in Fig. 10., there are multiple swarm configurations with a large number of nodes that yield a 24 hour satisfaction period. This corresponds to the flat plane at 24 hr satisfaction mark. As the number of nodes or the number of planes decreases, the plateau decays to 0. The swarms with 0 satisfaction period indicate that the target grid is not observed entirely by at least 2 nodes. The minimum sized swarm is then determined by noting the least number of nodes, T, before the plateau starts to decay.

- Minimum sized swarm: At $h_1 = 1660$ km, the minimum sized swarm consists of $T_1 = 180$ nodes consiting of 15 planes and 12 nodes per plane.
- Spacecraft lifetime: The spacecraft's orbital life due to perturbations from aerodynamic drag and SRP are noted from STK. It is found that a 3U CubeSat with specifications mentioned in Table 4 does not decay from this altitude within 10^5 Orbits.
- Station keeping ΔV: The ΔV required to maintain the orbit for 1 year, found from (8), is about 0.005 m/s.
- Performance under single point failure: The performance under single point failure is simulated by eliminating one of the nodes in the constellation. The simulations showed that the swarm is able to observe the entire target area. However, the duration of satisfaction decayed by about 3.8 hrs per day.

Minimal constellation at $h_2 = 1240$ km: The response of the satisfaction duration of multiple swarms possible at $h_2 = 1240$ km is presented in Fig. 11. The design space of N_p and N_{sp} was also limited to the range $[10, 18]$. The constellation performance is noted as follows.
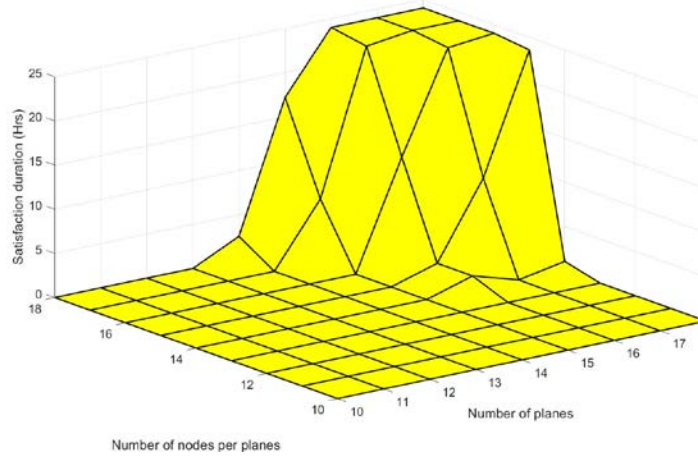

Fig. 11. Satisfaction duration of the multiple swarms possible at $h_2 = 1240$ km.

- Minimum sized swarm: At $h_2 = 1240$ km, the minimum sized swarm consists of 2 configurations, each consisting of $T_2 = 288$ nodes: One with $N_p = 16, N_{sp} = 18$ and the other one with $N_p = 18, N_{sp} = 16$.
- Spacecraft lifetime: The lifetime analysis showed that decay of the spacecraft's orbit due to drag and SRP is slow, and does not decay within 10^5 Orbits.
- Station keeping ΔV: The ΔV required to maintain the orbit for 1 year is about 0.024 m/s.
- Performance under single point failure: The simulations showed that under a single point failure, the swarm is able to observe the entire target area. However, the swarm with $N_p = 16$ lost coverage for 2.5 hrs, while the coverage of the swarm with $N_p = 18$ decayed by 2.4 hrs.

Minimal constellation at $h_3 = 871$ km: The response of the satisfaction duration of multiple swarms possible at $h_3 = 871$ km is presented in Fig. 12. The design space of N_p and N_{sp} was limited to the range $[18, 25]$. The constellation performance is noted as follows:
- Minimum sized swarm: At $h_3 = 871$ km, the minimum sized swarm consists of $T_3 = 525$ nodes consiting of 25 planes and 21 nodes per plane.
- Spacecraft lifetime: The lifetime analysis showed that decay of the spacecraft's orbit due to drag and SRP is slow, and does not decay within 10^5 Orbits.
- Station keeping ΔV: The ΔV required to maintain the orbit for 1 year is about 0.14 m/s.
- Performance under single point failure: The simulations showed that the swarm is able to observe the entire target area. However, the duration of satisfaction decayed by about 1.7 hrs per day.
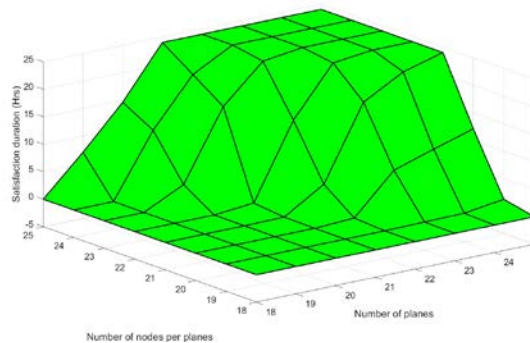

Fig. 12. Satisfaction duration of the multiple swarms possible at $h_3 = 871$ km.

Minimal constellation at $h_4 = 544$ km: The response of the satisfaction duration of multiple swarms possible at $h_4 = 544$ km is presented in Fig. 13. The design space of N_{sp} was limited to the range $[40, 32]$, and to the range $[40, 35]$ for N_p. The choice for this design space was because, the number of satellites significantly increased in this design and thus increasing the computation time. However, the minimal swarm still corresponds to the least number of nodes possible at this altitude, as the plateau decays are observed as the parameters are reduced in magnitude as seen in Fig. 13. The constellation performance is noted as follows and
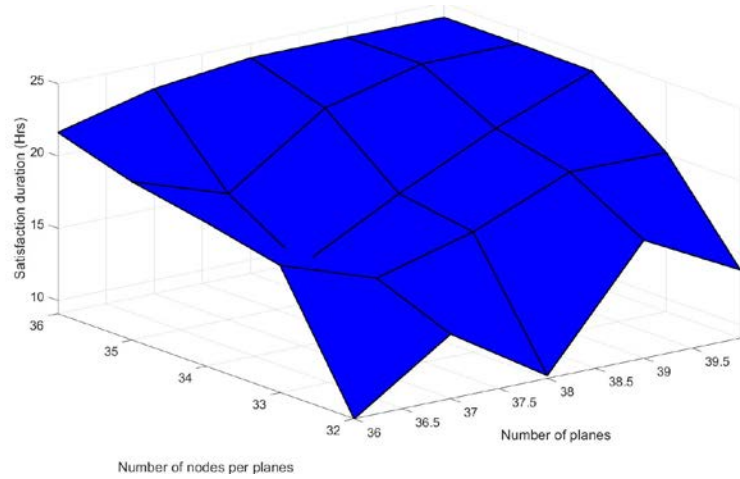

Fig. 13. Satisfaction duration of the multiple swarms possible at $h_4 = 544$ km.

- Minimum sized swarm: Similar to h_2, two swarm configurations of $T_4 = 1406$ nodes are possible at $h_4 = 544$ km: One configuration with $N_p = 37, N_{sp} = 38$ and another one with $N_p = 38, N_{sp} = 37$.
- Spacecraft lifetime: The lifetime analysis showed that the altitude of the orbit lifetime is about 7.4 years.
- Station keeping ΔV: The ΔV required to maintain the orbit for 1 year is about 6.9 m/s.
- Performance under single point failure: The simulations showed that under a single point failure, the swarm is able to observe the entire target area as well. However, the swarm with $N_p = 37$ lost the coverage for 0.86 hrs, while the coverage of the swarm with $N_p = 38$ decayed by 0.97 hrs.
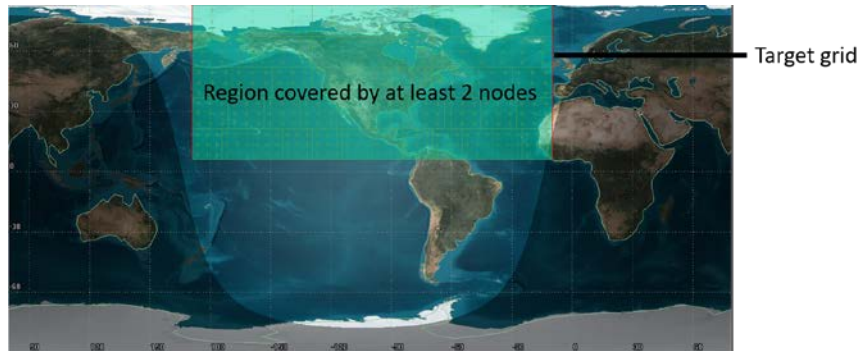

Fig. 14. Regional coverage of swarm constellation shown for the design at altitude, $h_1 = 1670$ km, showing 100 % regional coverage by 2 at least 2 satellites.

The results of these 4 swarms are summarized in Table 5. Each of these minimal swarm was able to provide 100% coverage continuously above North America. The coverage plot of the swarm constellation at $h_1 = 1660$ km is presented in Fig. 14 as a map plot, as an example. The turquoise shaded region presents the portion of the grid for which 2 satellite coverage is possible, while the grid itself is marked in red. The plots of all the 4 swarm designs are presented in Fig. 15.

Table 5. Summary of results of the 4 constellations designed.

h [km]	N_p	N_{sp}	T	Orbital life, if applicable [years]	Station keeping ΔV [(m/s) /year]	Coverage decay from single node failure [hrs/day]
1660	15	12	180	No	0.005	3.8
1240	16	18	288	No	0.024	2.5
	18	16				2.4
871	25	21	525	No	0.14	1.7
544	37	38	1406	7.4 years	6.9	0.86
	38	37				0.97

It can be seen from Table 5. that as the operational altitude of the swarm increases, the number of nodes required for the required coverage decreases. This pattern agrees with (5), since as the h increases, ρ decreases in magnitude, which indicates that the spacecraft can observe larger portions of the target region than at lower altitudes, therefore fewer nodes are required to observe the target region. A consequence of this is that the coverage decay in case of single point failures is more at these altitudes as seen in Table 5. Another added advantage of the higher altitude orbits is that the absence of atmosphere makes the nodes maintain their orbits for longer times than lower altitude orbits, and therefore the station keeping ΔV is also less at these altitudes. A key point to be observed is that all the 4 configurations were able to observe the complete target area with atleast 2 spacecrafts, which suggests that a swarm constellation is well placed to withstand single point failures.

Therefore, a minimum sized swarm can be deployed at any of the 4 RGT altitudes mentioned above. The RGT condition ensures that their orbit pattern repeats every day. Deploying the swarm at higher LEO altitudes can ensure long life and minimal station keeping. On the other hand, low altitude orbits in LEO require more fuel but are more tolerable to single point failures. At this point in the design, additional mission constraints such as launch costs, and ground station constraints can further constrain the specific operating altitude.
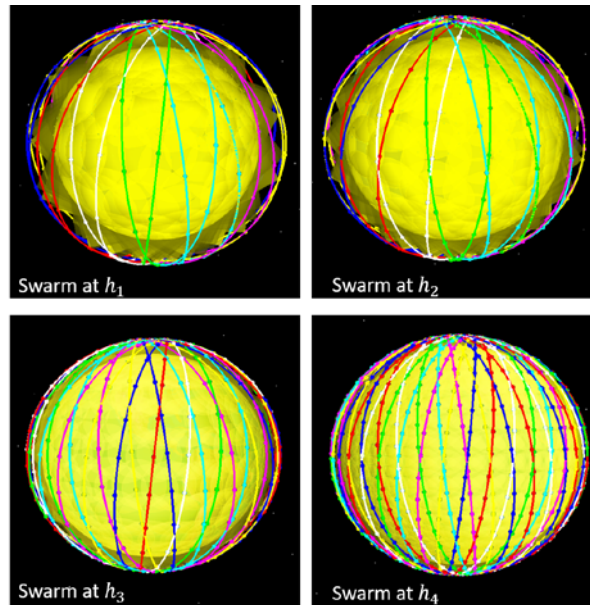

Fig. 15. Plots of the 4 swarm constellations presented in Table 5. The yellow region over the surface of the Earth is the field of view of each spacecraft. For the altitudes where 2 configurations are possible, the configuration of the minimum number of planes is presented.

5. CONCLUSION

In this work, we determined a minimum-sized swarm constellation to observe meteor trails above all of North America. The nodes of the swarm are the SWIMSat spacecraft, which is a proposed 3U CubeSat that uses onboard vision processing to detect meteor trails. Having a swarm enables multipoint observations of the meteor trails, which then allows us to triangulate the position of meteors in real-time and learn valuable insights into their origin and physical properties. With this in mind, the work focused on the problem of designing the swarm constellation in LEO such that it can continuously monitor an altitude of 140 km above all of North America using 2 nodes at any one time. The work uses computational tools and routines developed in STK and MATLAB to design the minimum sized swarm at each altitude. First, the orbit of the seed node was decided, such that the inclination maximized the target area observed, and the altitude guaranteed that the orbit tracks would repeat every day. Then the coverage performance of multiple swarms was studied by varying the constellation parameters, from which the minimum sized swarm was noted based on the satisfaction duration. Finally, key practical constraints such as orbital life, station keeping, and performance under single point failures are noted. The results identified 4 minimum sized swarms each corresponding to a different operating altitude. The larger altitudes require fewer spacecrafts and can be expected to have long orbital life, while the swarm in lower altitude suffer from lower decay in coverage period. All 4 designs were able to observe the complete target area even when there was a single node failure, which shows that the swarms can readily withstand single point failures.

6. REFERENCES

1. Popova, Olga P., et al. "Chelyabinsk airburst, damage assessment, meteorite recovery, and characterization." *Science* 342.6162 (2013): 1069-1073.
2. "Fireball and Bolide Data." NASA, NASA, cneos.jpl.nasa.gov/fireballs
3. Hernandez, V., Gankidi, P., Chandra, A., Miller, A., Scowen, P., Barnaby, H., Adamson, E., Asphaug, E., Thangavelautham, J. "SWIMSat: Space Weather and Meteor Impact Monitoring using a Low-Cost 6U CubeSat." (2016).
4. Nallapu, R., Ravindran, A., Kalita, H., Hernandez, V., Reddy, V., Furfaro, R., Asphaug, E., Thangavelautham, J., "Smart camera system onboard a CubeSat for space-based object reentry and tracking." *Position, Location, and Navigation Symposium (PLANS), 2018 IEEE/ION*. IEEE, 2018.
5. Murad, Edmond, and Iwan P. Williams, eds. *Meteors in the Earth's Atmosphere: Meteoroids and Cosmic Dust and Their Interactions with the Earth's Upper Atmosphere*. Cambridge University Press, 2002.
6. Hawkes, R. L. "Video-based meteor observation procedures." *WGN, Journal of the International Meteor Organization* 18 (1990): 152-158.
7. Ceplecha, Zdenek. "Geometric, dynamic, orbital and photometric data on meteoroids from photographic fireball networks." *Bulletin of the Astronomical Institutes of Czechoslovakia* 38 (1987): 222-234.
8. Pecina, P., and Z. Ceplecha. "New aspects in single-body meteor physics." *Bulletin of the Astronomical Institutes of Czechoslovakia* 34 (1983): 102-121.
9. Vallado, David A., and Wayne D. McClain. *Fundamentals of Astrodynamics and Applications*. 4th ed., Microcosm Press, 2013.
10. Wertz, James Richard. "Mission geometry: orbit and constellation design and management: spacecraft orbit and attitude systems." *Mission geometry: orbit and constellation design and management: spacecraft orbit and attitude systems/James R. Wertz. El Segundo, CA; Boston: Microcosm: Kluwer Academic Publishers, 2001. Space technology library; 13* (2001).
11. Wertz, James R., David F. Everett, and Jeffery J. Puschell. *Space mission engineering: the new SMAD*. Microcosm Press, 2011.
12. Luo, Xin, et al. "A novel technique to compute the revisit time of satellites and its application in remote sensing satellite optimization design." *International Journal of Aerospace Engineering* 2017 (2017).
13. Sandau, Rainer, Klaus Brieß, and Marco D'Errico. "Small satellites for global coverage: Potential and limits." *ISPRS Journal of Photogrammetry and Remote Sensing* 65.6 (2010): 492-504.
14. Tan, T., and F. Yang. "Hj-1a/1b constellation orbit design." *Spacecraft Engineering* 18.6 (2009): 27-30.